Doubly Fed Induction Generator Wind Turbine Control Based on a Novel MRAS Observer

Oluwaseun Simon Adekanle, M. Guisser, E. Abdelmounim, M. Aboulfatah, H. Bahri

Laboratory of System Analysis and Information Processing
Université Hassan 1er
Settat, Morocco
adekanlesimon@gmail.com

Adeola Balogun

Department of Electrical and Electronic Engineering
University of Lagos
Lagos, Nigeria
balog975@yahoo.com

Abstract. This paper proposes a novel Doubly Fed Induction Generator (DFIG) control approach using an optimized set of observers. Firstly, an Adaptive Disturbance Rejection Scheme (ADRS) Model Reference Adaptive System (MRAS) observer is applied to estimate generator speed. Secondly, a Fuzzy Logic MPPT controller is designed to optimized power conversion. Finally to achieve the overall sensor-less control, speed, current and DC-voltage control are achieved using a novel version of perturbation observer while taking into account the power loss in the system. The technique is evaluated for a 1.5MW DFIG under variable wind speed, measurement noise, grid voltage dip and parameter variation and compared with the conventional PI-controller.

Keywords: ADRS, Integral Backstepping Control, DFIG Control, MRAS, Fuzzy Logic, MPPT, Extended State Observer, Crowbar, DC-chopper.

1 Introduction

The purpose of Maximum power Point Tracking (MPPT) is to optimize the operation of the wind turbine to capture the maximum power possible. The first approach is the technique using relative velocity, which aims to control the speed of rotation of the generator to keep the relative speed at its optimum value [1]. This method requires a perfect knowledge of the parameters of the turbine and the measurement of the wind speed. Meanwhile, the use of a single anemometer leads to a local measure of wind speed that is not representative of the effective wind speed incident on the blades. Thus, an erroneous measurement of the wind speed leads to a degradation of the extracted power. To solve this problem of wind speed measurement, some researchers have worked on the estimation of wind speed using different techniques. Song et al in [2] proposed and compared two methods of wind speed estimation using different versions of the Kalman filter. The inconvenience of this methods resides in the fact that Kalman filters are complex and require high number of tuning parameters. In addition the stability of these estimator is not verified in close loop with controllers to achieve the complete control of the DFIG wind turbine. Belmokhtar et al in [3] developed a Fuzzy Logic based technique to estimate

ICCWCS 2019, April 24-25, Kenitra, Morocco

DOI 10.4108/eai.24-4-2019.2284107

wind speed and control the DFIG in close loop. However, stability analysis is not given. The second method for extracting the maximum wind power is by the Perturbation and Observation technique which is often used in the photovoltaic system [4]. It is easy to implement, less expensive and requires neither the knowledge of turbine parameters nor the measurement of wind speed [5]. However, this algorithm does not give good convergence because we have to make a compromise between the speed of convergence and performance. Other versions were then proposed such as neural network, gradient methods to give better performances but are still difficult to implement [1]. Optimal Torque Control (OTC) is a method which consists in adapting the electromagnetic torque (or power) to its optimum value without the need to measure wind speed. The disadvantage of this OTC technique is that characterization tests are required off-line to design the look-up table. In general, the OTC method is unsuitable for medium and large wind turbines because their inertia slows down the response during abrupt or rapid changes in wind speed [6]. We propose therefore a method based on Fuzzy Logic maximum power point search algorithm which is independent of wind speed measurement and which indirectly takes power loss in the system into consideration. It depends solely on the measurement of generator speed and output power.

Many controllers like PI-controller [7], Sliding Mode Controller [8], Backstepping [9], Model Predictive Control [10], and Fuzzy Logic Controller [11] have been successfully designed to control generator speed and currents in order to extract maximum power from the DFIG turbine through Maximum Power Point Tracking (MPPT) Techniques. They are equally employed to optimize the exchange of electrical energy between the turbine and the utility grid through Unity Power Factor (UPF) control. These controllers are synthesized assuming that all variables needed by the control algorithm are measurable from material and economic point of view. However, using mechanical, current and voltage sensors increases the cost of both equipment and maintenance, and reduces the reliability of the overall wind turbine system because they are prone to measurement noise and faults. Several techniques to observe one or more variables of the wind turbine system have been proposed in the literature. The authors in [12] proposed a Luemberger observer to estimate rotor currents from voltage, speed and power measurements. Only the RSPC control strategies is presented and the measurement of generator speed reduces the efficiency of the overall system. In [13] a modified PLL is employed to estimate generator speed but presented results show slow convergence of the estimator-controller. A Fuzzy-MRAS generator speed observer is elaborate in [3] but the stability and convergence of the Fuzzy adaptive mechanism with 25 rules are not proven.

In this paper an ADRT-based MRAS observer through modified Nonlinear Extended State Sliding Mode Observer and Lyapunov stability theory is proposed to observe generator speed. The observer takes into account only stator voltage measurement and observed rotor currents.

The control of the DFIG by stator flux orientation[14] stator voltage [15] or air gap flux [16] is a technique synthesized by assuming that the grid voltage is ideal and the stator flux is constant or vary very slowly. However, stator flux introduces high nonlinearity into the system during network fault. In fact, the variation of the stator flux during grid voltage drop depends on the value of the stator flux at the instance of occurrence and an exponential term [17]. Other authors like *Bhattarai et al.* [18] have proposed the use of stator and current measurements to estimate the flux in open loop. However, the accuracy of the flux estimation depends strongly on the machine parameters. If grid voltage dip occurs, the control laws cannot therefore respond directly and quickly to contain the disturbances generated by flux estimation incertitude and nonlinearity during fault moments. This causes degradation of the performance of these controllers during the voltage drop.

In this paper, an adaptive technique based on disturbance rejection is proposed to control the speed of the DFIG, rotor current-, filter current and the DC bus voltage. It consists of estimation followed by compensation, in real time, of network disturbances, parameter variation, modeling error and the decoupling terms. It is a simple and unique controller design method that has been proposed by Han [6] and improved by Gao [7]. This observer-controller has shown an apparent efficiency and a robust performance even without the exact knowledge of the system parameters.

2 ADRS control

Fig. 1 illustrates the complete proposed observer-based Fuzzy MPPT disturbance rejection control of the DFIG wind turbine. Fuzzy MPPT controller extracts optimal generator reference speed that leads to the maximization of extracted power. Two control objectives are intended to be carried out by the ADRS technique: tracking of the reference speed and desired stator reactive power. The MRAS observer estimates the actual generator speed from current measurement and supplies it to the controller. At the GSPC, the control objective is to keep the DC bus voltage constant at its nominal value and annul the reactive power generated by the filter.

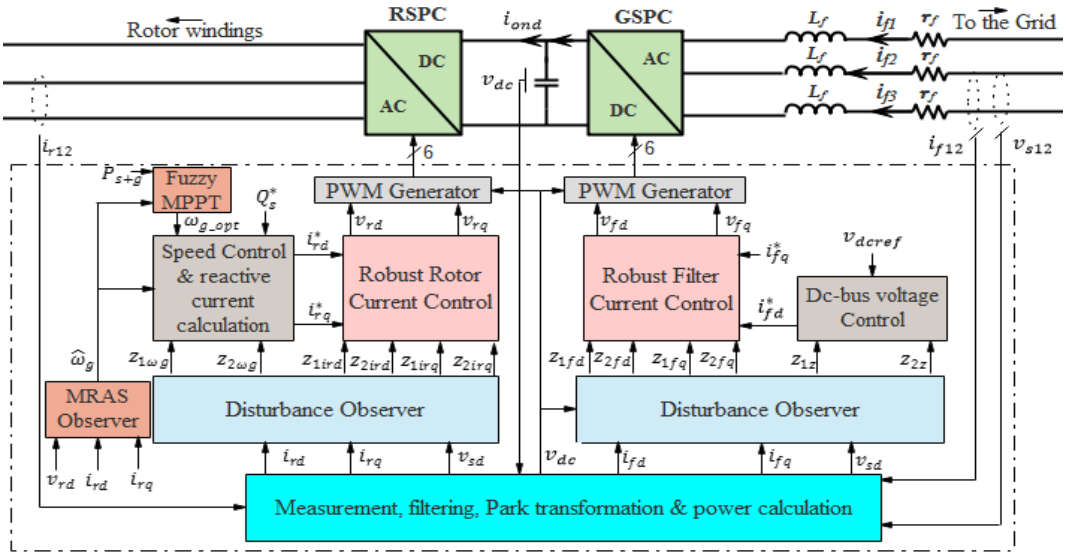

Figure 1 : Synoptic diagram of the overall control structure.

2.1 MRAS Speed Observer

The proposed MRAS speed estimator consists of a reference model (available variable) and an adaptive model (equation of the available model with $\widehat{\omega}_g$ as variable to be estimated) as illustrated in fig. 2. The error between both models is driven to zero by an adaptation mechanism based on a simple Adaptive Disturbance Rejection Scheme (ADRS). The output of the reference model v_{rd} is easily accessible at the output of RSPC controller. The adaptive model under stator voltage orientation control is obtained from voltage and flux equations [19] and expressed in (1).

$$\hat{v}_{rd} = \sigma L_r \frac{di_{rd}}{dt} + R_r i_{rd} - \sigma L_r(\omega_s - \hat{\omega}_g) i_{rq} - (\omega_s - \hat{\omega}_g) \frac{L_m \omega_s \varphi_{sq}}{L_s} \quad (1)$$

Fig. 3 describes the ADRS adaptive mechanism technique applied to reduce the error between the reference and adaptive models. If the parameters of the controller are carefully chosen, the error between the reference v_{rd} and adaptive $\hat{v}_{rd}$ models converges to zero and the controller output is the estimate of the DFIG rotational speed. The main advantage of using ADRS as adaptation mechanism is its robustness and high precision. This technique is chosen because it does not require knowledge of the dynamics of the adaptive model. It is based solely on the consideration of the adaptive model as having a general form described by (2), where θ is an unknown variable, b is a control constant and $\hat{\omega}_g$ is the variable to be observed.

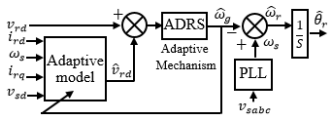

Figure 2 : MRAS speed observer technique.

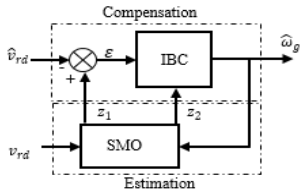

Figure 3 : MRAS Adaptive mechanism.

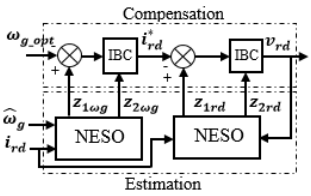

Figure 4 : Disturbance observer and compensation for speed and current control.

$$\frac{dv_{rd}}{dt} = b\hat{\omega}_g + \theta(\omega_s, \varphi_{sq}, i_{rd}, i_{rq}) \quad (2)$$

The first step in the convergence of $\hat{v}_{rd}$ to v_{rd} is then the determination of the unknown variable θ in order to be able to synthesize an appropriate control law. The solution then is to develop an observer to construct θ from v_{rd}. An observer for the system described by (2) is the optimized Sliding Mode Observer (SMO) presented in (3).

$$\begin{cases} \dot{z}_1 = z_2 + b\hat{\omega}_g + \rho_1 \left(|e|^{\alpha_1} sign(e) + |e|^{\beta_1} sign(e) \right) + k_1 sign(e) \\ \dot{z}_2 = \rho_2 \left(|e|^{\alpha_2} sign(e) + |e|^{\beta_2} sign(e) \right) + k_2 sign(e) \\ e = \hat{v}_{rd} - z_1 \end{cases} \quad (3)$$

where : z_1 and z_2 are the estimations of $\hat{v}_{rd}$ and θ respectively. The constants ρ_1, ρ_2, α_1, α_2, β_1, β_2, k_1, k_2 are the adjustment parameters of the observer. Equation (4) is substituted into (3) in order to avoid chattering.

$$sign(e) = \begin{cases} 2\left(\frac{1}{1 + exp^{-\tau e}} - \frac{1}{2}\right), & |e| \leq \delta \\ sign(e), & |e| > \delta \end{cases} \quad (4)$$

Once the estimate of the unknown variable is available, it remains to synthesize a control technique for the tracking of the reference model. After the observation, the dynamics of $\hat{v}_{rd}$ becomes (5). Application of Integral Backstepping Control thus gives (6).

The slip speed ω_r is calculated from the stator angular speed ω_s extracted by the PLL and the observed rotor speed $\widehat{\omega}_g$ as ($\omega_r = \omega_s - \widehat{\omega}_g$). A simple integral action on the observed rotor angular speed is applied to obtain the angle for Park transformation of stator variables.

$$\dot{z}_1 = z_2 + b\widehat{\omega}_g \tag{5}$$

$$\widehat{\omega}_g = \frac{1}{b}\left(-k\varepsilon - z_2 + \dot{v}_{\mathrm{rd}} - k_i(z_1 - v_{\mathrm{rd}})\right) \tag{6}$$

2.2 Non Linear Extended State Observer

Here we propose a real time estimation and compensation of the coupling terms as well as other disturbances that may occur in the system due to parameter variation, measurement noise or grid voltage dip. To proceed, we take the disturbance into account in speed, current and DC voltage dynamics as expressed in (7). The disturbance, in form of parametric incertitude, flux nonlinearity or modelling error, is represented as a lumped parameter $\emptyset$ in speed, rotor, filter and DC bus mathematical models. The lumped parameter, the coupling terms as well as the nonlinearity in the models are considered as a generalized disturbance ($z_{2\omega g}$, z_{2rd}, z_{2rq}, z_{2z}, z_{2fd}, z_{2fq}). Expressions of rotor, filter and DC bus models are hence reduced and presented in (7) where ($z_{1\omega g}$, z_{1rd}, z_{1rq}, z_{1z}, z_{1fd}, z_{1fq}) represent (ω_g, i_{rd}, i_{rq}, z, i_{fd}, i_{fq}).

$$\begin{cases} \dfrac{dz_{1\omega g}}{dt} = uz_{1rd} + z_{2\omega g} \\ \dfrac{dz_{1rd}}{dt} = b_r v_{rd} + z_{2rd} \\ \dfrac{dz_{1rq}}{dt} = b_r v_{rq} + z_{2rq} \end{cases} \qquad \begin{cases} \dfrac{dz_{1fd}}{dt} = b_f v_{fd} + z_{2fd} \\ \dfrac{dz_{1fq}}{dt} = b_f v_{fq} + z_{2fq} \\ \dfrac{dz_{1z}}{dt} = b_z z_{1fd} + z_{2z} \end{cases} \tag{7}$$

The generalized disturbances in form of extended states are:

$$\begin{cases} u = -\dfrac{3}{2}p\dfrac{L_m}{JL_s}\varphi_{sq} \\ z_{2\omega g} = \left(C_m - f_v\omega_g + \emptyset_{\omega g}\right)/J \\ z_{2rd} = -\dfrac{R_r i_{rd}}{\sigma L_r} + \omega_r i_{rq} + \dfrac{L_m\omega_r\varphi_{sq}}{\sigma L_r L_s} + \emptyset_{rd} \\ z_{2rq} = -\dfrac{R_r i_{rq}}{\sigma L_r} - \omega_r i_{rd} + \emptyset_{rq} \\ b_r = \dfrac{1}{\sigma L_r} \end{cases} \qquad \begin{cases} z_{2fd} = -\dfrac{R_f}{L_f}i_{fd} + \omega_s i_{fq} + \dfrac{v_{sd}}{L_f} + \emptyset_{fd} \\ z_{2fq} = -\dfrac{R_f}{L_f}i_{fq} - \omega_s i_{fd} + \emptyset_{fq} \\ z_{2z} = \left(-P_{l_{filtre}} - P_{l_{CPCR}} - v_{dc}.i_{ond}\right)/C \\ \quad +\emptyset_z \\ b_f = \dfrac{-1}{L_f} \\ b_z = \dfrac{3v_{sd}}{2C} \end{cases}$$

2.2.a Disturbance Observers

A Nonlinear Extended State Observer (NESO) for the system (dynamiccs of $z_{1\mathrm{rd}}$ for example) describe by (7) can be expressed as:

$$\begin{cases} \dot{\hat{z}}_{1\mathrm{rd}} = \hat{z}_{2\mathrm{rd}} + bv_{rd} + \rho_1 \left(|e|^{\alpha_1} sign(e) + |e|^{\beta_1} sign(e) \right) + k_1 sign(e) \\ \dot{\hat{z}}_{2\mathrm{rd}} = \rho_2 \left(|e|^{\alpha_2} sign(e) + |e|^{\beta_2} sign(e) \right) + k_2 sign(e) \\ e = z_{1\mathrm{rd}} - \hat{z}_{1\mathrm{rd}} \end{cases} \quad (8)$$

If the observer parameters are judiciously chosen, e converges to zero therefore $\hat{z}_{1\mathrm{rd}}$ and $\hat{z}_{2\mathrm{rd}}$ are estimates of $z_{1\mathrm{rd}}$ and $z_{2\mathrm{rd}}$ respectively. In order to reduce the chattering phenomenon of the Sliding Mode Observer caused by the sign function, a super twisting algorithm is substituted into (8) where the sign function is replaced with the expression in (9). τ is a parameter inversely proportional to δ.

$$sign(e) = \begin{cases} 2\left(\frac{1}{1+exp^{-\tau e}} - \frac{1}{2}\right), & |e| \leq \delta \\ sign(e), & |e| > \delta \end{cases} \quad (9)$$

A careful study of the observer in (8) by [20] proposed a technique for determining the parameters of the NESO and it is applied in this paper as follows $1 < \rho_1, \rho_2 < +\infty$, $0.5 < \alpha_1 < 1$, $\alpha_2 = 2\alpha_1 - 1$, $\beta_1 = 1/\alpha_1$, $\beta_2 = \beta_1 + (\alpha_1 - 1)$ and $k_2, k_2 > 0$.

2.2.b Disturbance compensation

A simple error feedback control can be used to converge the current to its reference value as used in [20]–[22]. The disadvantage of this method is that the observation error is not taken into account in the command. This increases the convergence time or introduces a static error between the current and its desired value. To improve on this, we will use a more robust control technique that will ensure quick convergence to desired values.
Reference speed value ω_{g_opt} is computed online by the Fuzzy MPPT controller and its tracking by the controller gives the d-axis rotor current reference i_{rd}^*. The desired DC-bus voltage V_{dcref} is the nominal value of 1150V (1 p.u) and its tracking by the controller gives the d-axis filter current reference i_{rq}^*. This consequently implies that $z_{ref} = V_{dcref}^2/2 = 0.5\mathrm{p.u}$ due to the change of variable between V_{dc} and z.

Step 1: to control the speed of rotation of the generator and the DC bus voltage to follow the optimal rotational speed ω_{g_opt} generated by the MPPT command and the reference voltage z_{ref} of the DC bus respectively, we define the tracking errors by (10).

$$\varepsilon_{\omega g} = \hat{z}_{1\omega g} - \omega_{g\_opt} + k_{i\omega} \int \left(\hat{z}_{1\omega g} - \omega_{g\_opt} \right) dt \quad (10)$$

$$\varepsilon_{rd} = \hat{z}_{1rd} - i_{rd}^* \quad (11)$$

For easy readability, we replace i_{rd}^* and $i_{fd}^*$with α_{rd} and α_{fd} respectively. Following the Integral Backstepping controller method procedures presented in [19], the final control variable that guarsnttes the convergence of the speed to its optimal value ω_{g_opt} is:

$$v_{rd} = \frac{1}{b_r}\left(-k_{rd}\varepsilon_{rd} - u\varepsilon_{\omega g} - \hat{z}_{2rd} + \dot{\alpha}_{rd}\right) \quad (12)$$

Fig. 4 illustrates the technique of disturbance observation and compensation by the Extended State Observer and the Integral Backstepping respectively for rotational speed tracking.

3 Simulation results

To verify the performance of the proposed technique (observer-controller in close-loop), we will present the simulation results under measurement noise and network voltage drop. Fig. 5 shows the wind speed profile with which the turbine blades are driven.

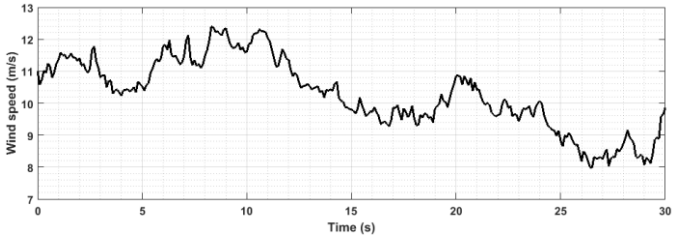

Figure 5 : Wind speed profile.

3.1 Simulation under Measurement Noise

In this paper, the effectiveness of the proposed technique is evaluated in the presence of measurement noises often introduced into the system by sensors. To achieve this, noise has been added, without filtering, to the measured variables that are not observed in this work. The distorted measurements (fig. 6) are then introduced to the control algorithm to synthesize the controller, the observers and the Fuzzy MPPT. For three-phase variables, only the first phases are presented for clarity but in simulation, the same noise is added to all the three phases.

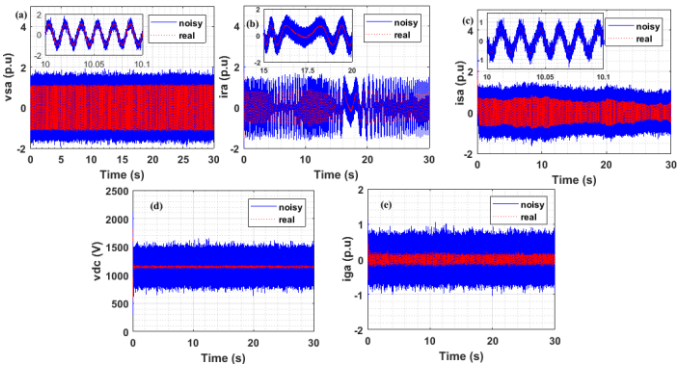

Figure 6 : System inputs with noise introduced.

Fig. 7.a shows the rotational speed, its estimate and the reference generated by the Fuzzy Logic MPPT controller. It is clear that despite the noisy inputs, the adaptive speed observer (MRAS), using the ADRS technique as an adaptation mechanism, rejects the noise and observes the speed with very good accuracy. We observe the same robustness on the normalized DC bus voltage (Fig. 7.b). The noises are rejected and the real state converges towards the reference (0.5 p.u). Fig. 7.c-f present the measured currents (currents coming from the noisy three-phase currents),

reference currents and the currents actually transmitted to the control algorithm by the observer. It is obvious that the disturbance observer rejects the noise and eliminates its effects on the control as the noisy currents are filtered by the observer. Reference currents are also noisy because they are generated from noisy quantities. However, the currents track their references while at the same time rejecting the noises.

Fig. 8 shows the output power, power coefficient and output currents of the wind turbine. We note that the active and reactive powers evolve without being disturbed by measurement noise. Likewise, the power coefficient evolves around the maximum possible efficiency of 50%. The currents follow wind speed profile without any overshoot above the nominal value of 1 p.u.

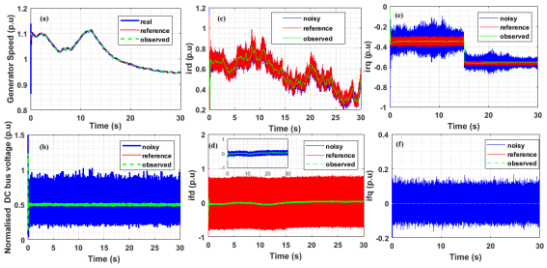

Figure 7 : Influence of observers on measurement noise

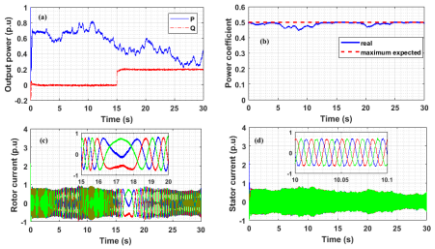

Figure 8 : DFIG output under noisy sensors.

3.2 Simulation under Deep Grid Voltage Dips

Simulations in this section are performed to verify and compare the capability of the proposed ADRS and PI-controller to satisfy the strictest scenario of LVRT requirement of the German grid code. According to the code, wind turbine generators are required to remain connected to the grid for at least 0.625s at the occurrence of grid voltage dip of up to 85%. A three-phase short-circuit fault is introduced to the grid at at the point of DFIG connection to the grid. The three phases of the grid voltage drop to 5% (95% dip) of their nominal values at t=10s and the dip lasts till t=10.625s.

Two DFIG protection schemes are included in the DFIG set-up. The first is the active crowbar which is activated when rotor current or DC bus voltage exceed their respective thresholds to limit inrush rotor current during fault. The second is the DC-chopper connected in parallel with the DC-link capacitor to limit DC voltage swell. It is activated at the same instance as the active crowbar. The deactivation of both protection circuits occurs simultaneously when both DC voltage and rotor current return below their thresholds. 1.35p.u and 1.2p.u are chosen as thresholds for DC voltage and rotor current respectively.

Fig. 9 shows that grid voltage is the same under both controllers, dips to 0.05p.u and its recovery is rapid with neither overshoot nor oscillations.

According to fig. 10.a, stator current overshoot poses no threat as it is limited below 1p.u at the instance of voltage rising under both controllers. However, significant stator current surge of 125% can be observed during voltage falling under PI-controller, which far exceeds admissible stator current. Under ADRS technique, stator current is limited around its admissible value of 1.2p.u during voltage rising.

In fig. 10.b, rotor current surge and settling are admissible during grid voltage recovery under both controllers as it is limited within the safe operating zone of the back-to-back converters. Unfortunately, rotor current evolution during voltage falling is identical to that of the stator current, it surges far above the save operating limit of the power converters up to 2.75p.u for the

PI-controller. The proposed approach using ADRS controller was able to keep the inrush current at 1.25p.u around the save operating area of the converters.
Comparing the DC voltage under PI and ADRS controllers, fig. 11 shows that the DC bus experienced a voltage swell during the network voltage drop under both controllers. Under control by the PI technique, the overvoltage exceeds 1.35p.u admissible for the safety of the DC bus and reaches 1.75p.u whereas under the control by ADRS, the surge reaches only 1.3p.u, which is just below the admissible voltage across the DC capacitor.

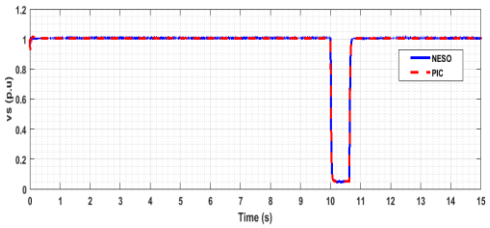

Figure 9: Grid voltage under short-circuit fault.

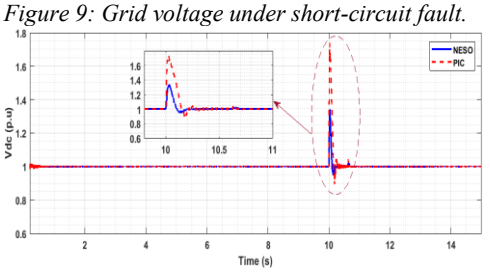

Figure 11 : DC-bus voltage under grid voltage dip.

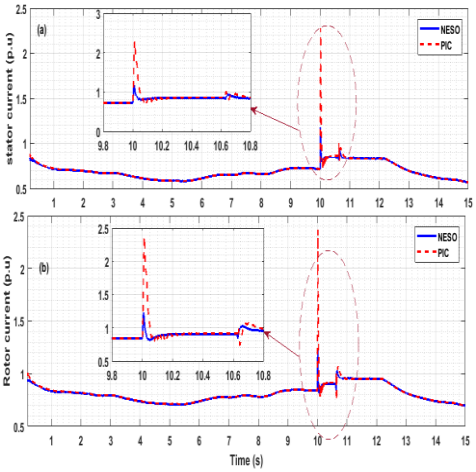

Figure 10: Stator and rotor currents under grid voltage dip.

Conclusion

The application of a novel MRAS observers in this paper does not only reduce the cost of installation, it also increases the reliability of wind turbine installations, eliminates measurement noise and reduces the complexity of control circuit setup

A precise measurement of the decoupling terms of the direct and quadrature components of the rotor currents and the filter is necessary for the good performance of the wind turbine control techniques. We have estimated decoupling terms by treating them as another state of the system. An IBC based on Lyapunov stability theory taking into account the integral of the error is then used for tracking current references.

The robustness the ADRS to measurement noise and grid fault has been demonstrated. The 1.5MW wind turbine connected to the infinite network is controlled by the PI and ADRS controllers. The comparative results under MATLAB / SIMULINK show that the ADRS is better able to reduce wind turbine rotor and stator overcurrent, thus increasing the safety level of bidirectional converters with respect to overcurrent caused by network voltage drop. In addition, the DC bus voltage is limited below its safe operating limit under control by ADRS, protecting the DC bus from overvoltage.

References

[1] M. A. Abdullah, A. H. M. Yatim, C. W. Tan, and R. Saidur, "A review of maximum power point tracking algorithms for wind energy systems," *Renew. Sustain. Energy Rev.*, vol. 16, no. 5, pp. 3220–3227, Jun. 2012.

[2] D. Song, J. Yang, M. Dong, and Y. H. Joo, “Kalman filter-based wind speed estimation for wind turbine control,” *Int. J. Control. Autom. Syst.*, vol. 15, no. 3, pp. 1089–1096, 2017.

[3] K. Belmokhtar, M. L. Doumbia, and K. Agbossou, “Novel fuzzy logic based sensorless maximum power point tracking strategy for wind turbine systems driven DFIG (doubly-fed induction generator),” *Energy*, vol. 76, pp. 679–693, 2014.

[4] C.-M. Hong, T.-C. Ou, and K.-H. Lu, “Development of intelligent MPPT (maximum power point tracking) control for a grid-connected hybrid power generation system,” *Energy*, vol. 50, pp. 270–279, Feb. 2013.

[5] L. Qu and W. Qiao, “Constant Power Control of DFIG Wind Turbines With Supercapacitor Energy Storage,” *IEEE Trans. Ind. Appl.*, vol. 47, no. 1, pp. 359–367, Jan. 2011.

[6] J. S. Thongam, M. Tarbouchi, R. Beguenane, A. F. Okou, A. Merabet, and P. Bouchard, “An optimum speed MPPT controller for variable speed PMSG wind energy conversion systems,” in *IECON 2012 - 38th Annual Conference on IEEE Industrial Electronics Society*, 2012, pp. 4293–4297.

[7] J. Ouyang, T. Tang, Y. Diao, M. Li, and J. Yao, “Control method of doubly fed wind turbine for wind speed variation based on dynamic constraints of reactive power,” *IET Renew. Power Gener.*, 2018.

[8] F. Zargham and A. H. Mazinan, “Super-twisting sliding mode control approach with its application to wind turbine systems,” *Energy Syst.*, no. 209, 2018.

[9] B. Bossoufi, M. Karim, A. Lagrioui, M. Taoussi, and A. Derouich, “Observer backstepping control of DFIG-Generators for wind turbines variable-speed: FPGA-based implementation,” *Renew. Energy*, vol. 81, pp. 903–917, 2015.

[10] A. Bektache and B. Boukhezzar, “Nonlinear predictive control of a DFIG-based wind turbine for power capture optimization,” *Int. J. Electr. Power Energy Syst.*, vol. 101, pp. 92–102, Oct. 2018.

[11] W. Ayrir, M. Ourahou, B. El Hassouni, and A. Haddi, “Direct torque control improvement of a variable speed DFIG based on a fuzzy inference system,” *Math. Comput. Simul.*, May 2018.

[12] R. Bhattarai, N. Gurung, A. Thakallapelli, and S. Kamalasadan, “Reduced-Order State Observer-Based Feedback Control Methodologies for Doubly Fed Induction Machine,” *IEEE Trans. Ind. Appl.*, vol. 54, no. 3, pp. 2845–2856, 2018.

[13] A. Giannakis, A. Karlis, and Y. L. Karnavas, “A combined control strategy of a DFIG based on a sensorless power control through modified phase-locked loop and fuzzy logic controllers,” *Renew. Energy*, vol. 121, pp. 489–501, Jun. 2018.

[14] N. Sarma, P. M. Tuohy, J. M. Apsley, Y. Wang, and S. Djurović, “DFIG stator flux-oriented control scheme execution for test facilities utilising commercial converters,” *IET Renew. Power Gener.*, vol. 12, no. 12, pp. 1366–1374, 2018.

[15] G. Calderón, J. Mina, J. C. Rosas-Caro, M. Madrigal, A. Claudio, and A. López, “Simulation and Comparative Analysis of DFIG-based WECS Using Stator Voltage and Stator Flux Reference Frames,” *IEEE Lat. Am. Trans.*, vol. 15, no. 6, pp. 1052–1059, 2017.

[16] S. Jing, N. Xiaohong, and L. Kean, “Air gap field-oriented vector control strategy for high-power electrically excited synchronous motor based on full-order flux linkage observer,” *Sci. Res. Essays*, vol. 9, no. 9, pp. 367–373, May 2014.

[17] M. Rahimi and M. Parniani, “Grid-fault ride-through analysis and control of wind turbines with doubly fed induction generators,” *Electr. Power Syst. Res.*, vol. 80, no. 2, pp. 184–195, Feb. 2010.

[18] R. Bhattarai, S. Member, N. Gurung, S. Member, and S. Ghosh, “Parametrically Robust Dynamic Speed Estimation Based Control for Doubly Fed Induction Generator,” *IEEE Trans. Ind. Appl.*, vol. PP, no. c, pp. 1–8, 2017.

[19] O. S. Adekanle, M. Guisser, E. Abdelmounim, and M. Aboulfatah, “Robust Integral Backstepping Control of Doubly Fed Induction Generator Under Parameter Variation,” *Int. Rev. Autom. Control*, vol. 10, no. 2, 2017.

[20] S. Xiong, W. Wang, X. Liu, Z. Chen, and S. Wang, “A novel extended state observer,” *ISA Trans.*, vol. 58, pp. 309–317, 2015.

[21] S. Gao, C. Mao, D. Wang, and J. Lu, “Dynamic performance improvement of DFIG-based WT using NADRC current regulators,” *Int. J. Electr. Power Energy Syst.*, vol. 82, pp. 363–372, 2016.

[22] Z. Song, T. Shi, C. Xia, and W. Chen, “A novel adaptive control scheme for dynamic performance improvement of DFIG-Based wind turbines,” *Energy*, vol. 38, no. 1, pp. 104–117, 2012.